

Microbial upcycling of plastic waste to levodopa

Received: 3 November 2024

Accepted: 4 February 2026

Published online: 16 March 2026

 Check for updates

Benjamin Royer¹, Yuta Era¹, Marcos Valenzuela-Ortega¹, Thomas W. Thorpe¹, Connor L. Trotter¹, Kitty Clouston¹, John F. C. Steele¹, Nicoll Zeballos¹, Eugene Shrimpton-Phoenix¹, Bhumrapee Eiamthong², Chayasith Uttamapinant², Christopher W. Wood¹ & Stephen Wallace¹✉

Using engineering biology to perform complex chemical synthesis offers a sustainable alternative to traditional processes that rely on finite fossil resources. A growing opportunity within this field lies in reclaiming carbon embedded in industrial and post-consumer waste—carbon otherwise lost to landfill, incineration or pollution. Here we report the bio-upcycling of poly(ethylene terephthalate) (PET) plastic waste into levodopa (L-DOPA), a frontline medication for Parkinson's disease, using engineered *Escherichia coli*. Two key bottlenecks—substrate import and feedback inhibition by the intermediate protocatechuate—were addressed through heterologous transporter expression and functional pathway separation across two microbial strains. To further improve sustainability, and as a proof-of-concept, *Chlamydomonas reinhardtii* was used to capture CO₂ released during catechol generation. The resulting bioprocess operates under mild, aqueous conditions and achieves high L-DOPA titres (5.0 g l⁻¹), with isolated product obtained at preparative scale from both industrial PET waste and a single post-consumer plastic bottle. This work demonstrates how engineering biology can transform plastic-derived aromatic monomers into high-value pharmaceuticals for the treatment of neurological disease in humans.

The modern chemical industry relies on the consumption of finite fossil resources at a pace and scale that is inherently unsustainable. These processes are energy intensive and generate consumer products that are ultimately disposed by landfill or incineration, resulting in the irretrievable loss of this valuable carbon as environmental pollution or CO₂ in the atmosphere. By contrast, nature has evolved elegant and efficient mechanisms for carbon resource utilization, by-product recycling and sustainable chemical synthesis. As these processes are genetically encoded, they offer a blueprint for modern engineering biology to remediate and upcycle carbon embedded in industrial and post-consumer waste. The resulting engineered bioprocesses can reintegrate this carbon into the circular chemical economy, while simultaneously reducing pollution, greenhouse gas emissions and the underlying drivers of global climate change.

Research in this area has focussed on the bioavailable polymers cellulose, chitin and lignin as substrates, but more recently has explored the use of plastic waste as a microbial feedstock. Enzymatic depolymerization of lignocellulose and chitin has yielded carbohydrate monomers for bacterial growth and upcycling pathways to biofuels¹, polyhydroxyalkanoates², terpenes³ and amino acids⁴, whereas aromatic monomers isolated from lignin have been used as cellular substrates for adipic acid⁵ and coniferyl alcohol⁶ synthesis. The bio-upcycling of plastic waste has been enabled by the discovery of enzymes capable of depolymerizing poly(ethylene terephthalate) (PET)⁷, catalysed by the discovery of *Ideonella sakaiensis*, a bacterium capable of depolymerizing and assimilating PET⁸. This breakthrough has since driven the engineering of IsPETase variants with enhanced catalytic performance for applications in industrial biotechnology (Fig. 1a). These efforts have

¹Institute of Quantitative Biology, Biochemistry and Biotechnology, School of Biological Sciences, University of Edinburgh, Edinburgh, UK.

²Vidyasirimedhi Institute of Science and Technology, Wangchan Valley, Rayong, Thailand. ✉ e-mail: stephen.wallace@ed.ac.uk

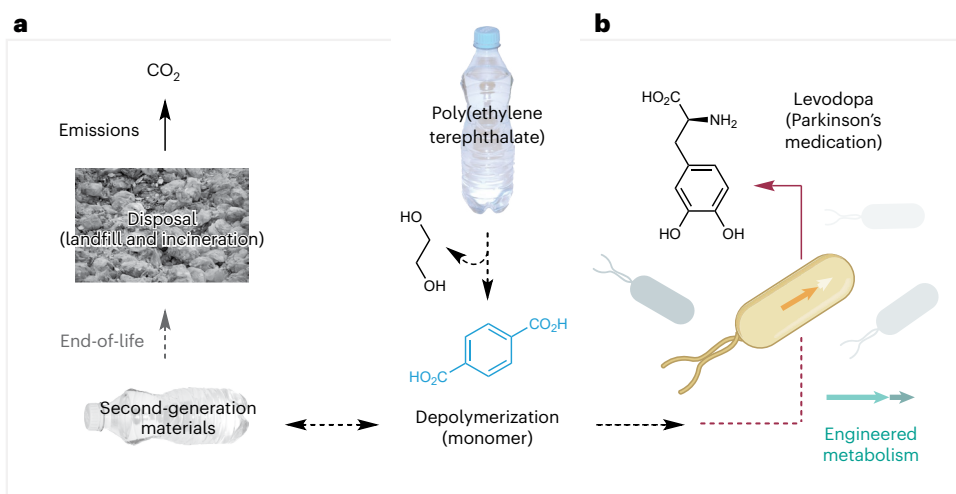


Fig. 1 | Plastic waste recycling and bio-upcycling strategies. Approaches to the recycling, upcycling and environmental disposal of PET plastic waste, including the proposed bio-upcycling of PET waste to the Parkinson's medication L-DOPA

in engineered bacteria. **a**, Current: closed-loop recycling. **b**, This work: microbial upcycling. Credit: photographs in **a**, Rawpixel (<https://www.rawpixel.com/>); bacterial icon in **b**, Bioicons (<https://bioicons.com/>).

yielded PET hydrolases with enhanced activity and thermal stability^{9,10}, as well as metabolic pathways for upcycling PET-derived monomers into value-added products such as vanillin¹¹, adipic acid¹², paracetamol¹³ and other platform chemicals^{14,15}. In addition, there exists a growing list of chemoenzymatic approaches to upcycle other plastic wastes such as poly(hydroxybutyrate) into acetone¹⁶, polyethylene into functionalized carboxylic acids¹⁷ and mixed plastic wastes into β -keto adipate and polyhydroxyalkanoates¹⁸. Chemical catalysts have also been interfaced with plastic upcycling pathways to create new biocompatible chemistry approaches and green synthetic chemistry methods¹⁹ for the mild conversion of a range of plastic wastes into industrially applicable second-generation chemical products. Of note, ref. 20 recently reported the use of chemical catalysis to convert post-consumer polystyrene to benzoic acid (Co(NO₃)₂ + Mn(NO₃)₂, *N*-hydroxyphthalimide, O₂ (4 bar), acetic acid, 150 °C followed by microbial conversion to the complex small molecules ergothioneine, mutilin and pleuromutinin in engineered *Aspergillus nidulans* and as a sole carbon source to generate the atoxigenic biocontrol agent *Aspergillus flavus* Af36. Similarly, another study¹⁸ coupled the chemocatalysed autooxidation of mixed domestic plastic wastes to oxygenated carboxylic acid intermediates with biotransformation by engineered strains of *Pseudomonas putida* KT2440 to create a metabolic funnel to valuable synthetic building blocks. Inspired by recent advances and the emerging potential of engineering biology to upcycle plastic waste into high-value molecules, we report the microbial conversion of industrial PET waste and a post-consumer PET plastic bottle into levodopa (L-DOPA), a frontline treatment for the symptoms of Parkinson's disease (Fig. 1b). L-DOPA is currently produced at a global scale of ~250 t yr⁻¹ (ref. 21) with demand projected to rise as a result of increased disease prevalence^{22,23}. Beyond its clinical importance, L-DOPA serves as a biosynthetic precursor to melanin and a variety of complex plant-derived natural products^{24,25}. Despite the existence of several biotechnological routes to L-DOPA—including fermentative pathways from L-tyrosine, chitin or D-glucose and expression in transgenic tomatoes—commercial production remains reliant on fossil fuel-derived chemical or chemoenzymatic synthesis^{26–30}. Each alternative faces notable challenges, such as poor carbon economy, oxidative degradation, inefficient feedstock utilization or regulatory hurdles. This work therefore offers a sustainable alternative to existing chemical and biological methods for producing L-DOPA from virgin petrochemicals and highlights the first application of engineering biology to valorize plastic waste into a therapeutic for neurological disease.

Results

De novo pathway design and optimization

L-DOPA synthesis from PET monomer terephthalic acid (TPA) was envisioned via a four-step biosynthetic pathway encoded by seven genes in the laboratory bacterium *Escherichia coli* BL21(DE3). The pathway proceeds via conversion of TPA to protocatechuate (PCA) catalysed by a terephthalate 1,2-dioxygenase complex (TphA2 and TphA3), and cognate reductase (TphA1; together referred as the TPADO complex) and dihydroxy-3,5-cyclohexadiene-1,4-dicarboxylic acid dehydrogenase (known as DCDDH or TphB) from *Comamonas* sp. Decarboxylation of PCA to catechol by AroY and prFMN cofactor regeneration enzyme KpdB from *Klebsiella pneumoniae* is then followed by a final C–C bond formation via electrophilic aromatic substitution between catechol and pyruvate in the presence of ammonia by the pyridoxal 5'-phosphate (PLP)-dependent tyrosine-phenol lyase (TPL) from *Fusobacterium nucleatum* to form L-DOPA (Fig. 2a). The *tpado* and *dcddh* genes were assembled on to a pGro7 derived backbone to generate pPCA1 (module 1), *aroY* and *kpdB* genes were assembled on to a pQLinkN vector to generate pCAT1 (module 2) and *tpl* was assembled in a joint universal modular plasmids (JUMP) assembly level 1 vector to generate *pFnTPL* (module 3). The activity of each module was examined by transforming *E. coli* BL21(DE3) cells with pPCA1, pCAT1, pPCA1 + pCAT1 or *pFnTPL*, confirming soluble protein expression after growth in LB medium by SDS-PAGE (Supplementary Figs. 1 and 2) and then incubating with the requisite pathway substrate or intermediate in a whole-cell biotransformation (optical density OD₆₀₀ = 30).

Cells containing TPADO-dcddh (module 1), AroY/KpdB (module 2) or TPL (module 3) enzymes were highly active in isolation and observed to convert >90% substrate to product in 24 h (Fig. 2b). We sought to improve diffusion of terephthalate across the negatively charged bacterial cell membrane. This is known to be most efficient at pH 5 (ref. 11) (pKa1 = 3.5; pKa2 = 4.3) and therefore to mitigate this at pH 7 we assembled *tpaK* from *Rhodococcus jostii* downstream of the *tpado* and *dcddh* genes via homologous end assembly to generate the modified plasmid pPCA3 (Supplementary Fig. 3). TpaK is part of the major facilitator superfamily class of membrane transporters and has been shown to import aromatic acids including TPA when heterologously expressed in *P. putida*^{31,32}. Pleasingly, TPA conversion to PCA at pH 7 displayed accelerated product formation (Fig. 2c). To our knowledge this constitutes the first use of a TPA transporter for biocatalysis in *E. coli*.

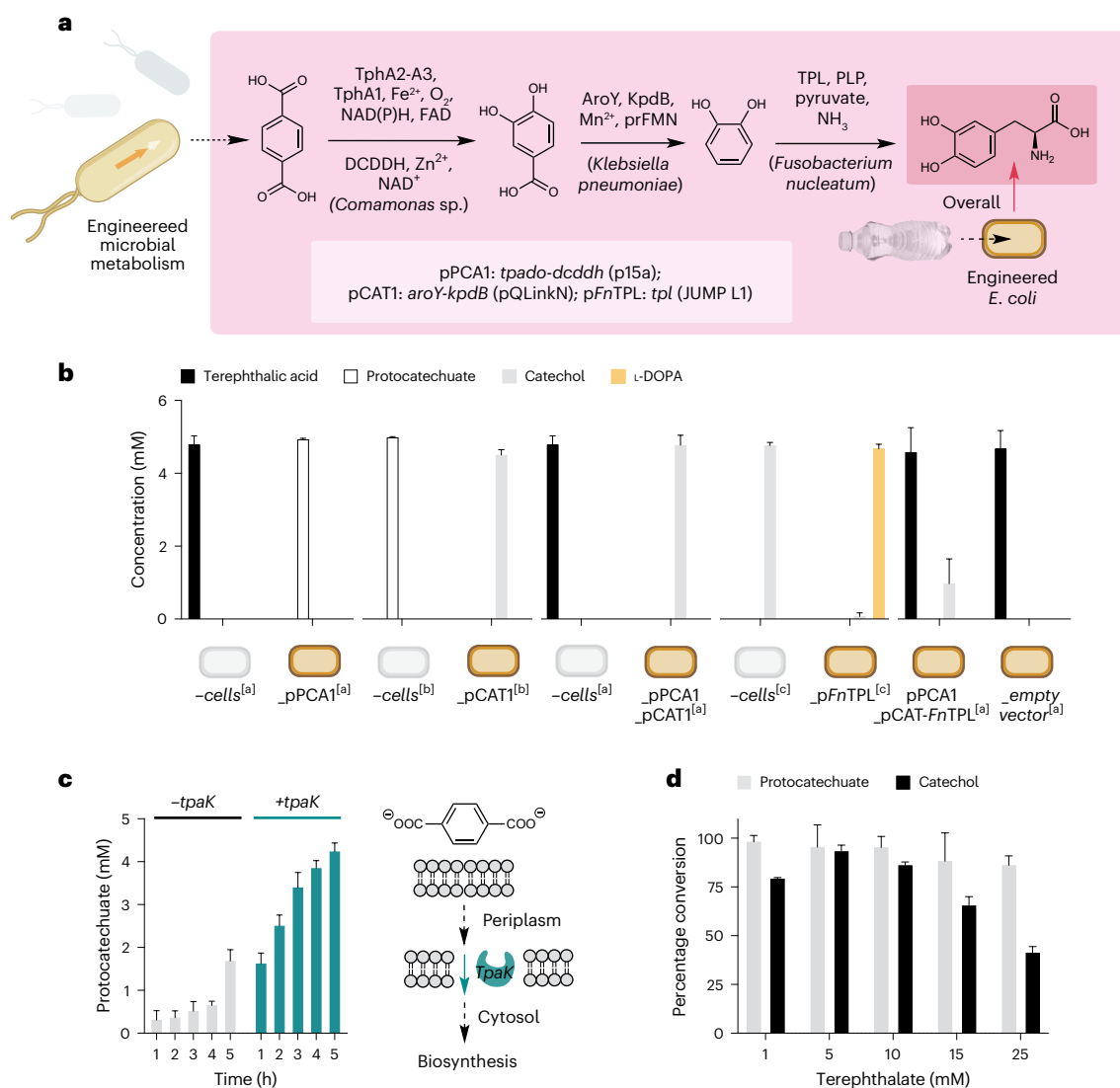


Fig. 2 | Pathway design, construction and bottlenecks. a, De novo biosynthetic pathway to L-DOPA from PET monomer TPA. **b**, Whole-cell activity when pPCA1, pCAT1 and pFnTPL are singly and multiply expressed in *E. coli* BL21(DE3) as well as whole pathway with pPCA1_pCAT-FnTPL. **c**, Enhanced TPA conversion to PCA in strains *E. coli*_pPCA1 and *E. coli*_pPCA3 expressing *tpaK* from *R. jostii*. **d**, PCA and catechol conversions upon increasing terephthalate concentration in strains *E. coli*_pPCA3 and *E. coli*_pPCA3_pCAT1, respectively. Metabolite

concentrations were determined by reverse-phase HPLC relative to an internal standard of caffeine (0.01 g l^{-1}). Data are presented as an average of three replicate experiments to one standard deviation. All data shown are from 3 ml reactions performed in 15 ml Falcon tubes. In **b**, the supercripts are as follows: ^[a]TPA substrate; ^[b]PCA substrate; and ^[c]catechol substrate. Credit: photograph in **a**, Rawpixel (<https://www.rawpixel.com>); bacterial icons in **a**, Bioicons (<https://bioicons.com>).

Co-transformation with pCAT1 generated the modified strain *E. coli*_pPCA3_pCAT1 for conversion of TPA to catechol. Despite high-level production of PCA by *E. coli*_pPCA3, conversion to catechol was efficient at low concentration (1–10 mM; >85%) but decreased to <40% with increasing TPA loading (Fig. 2d). Intriguingly, the addition of 30 mM catechol also resulted in a dramatic reduction in conversion of TPA to PCA in this strain, indicating that catechol inhibits TPADO activity at this concentration (Supplementary Fig. 5). Although the precise mechanism of inhibition is unclear, preliminary molecular docking simulations indicated favourable binding interactions between catechol and TPADO in and around the active site and *ortho*-quinone formation under the oxygenic conditions required for TPA conversion to PCA could covalently inhibit TPADO or compete for Fe binding within the active site. Additionally, catechol is known to inactivate proteins through cross-linking and has been shown to inhibit reductases^{33,34}. Regardless, it was hypothesized that catechol mediated TPADO inhibition would be limited through conversion to L-DOPA within the full biosynthetic pathway.

Pathway inhibition and in silico modelling

To circumvent the accumulation of catechol in whole-cell reactions containing TPADO, *E. coli*_pPCA1 was transformed with pCAT-FnTPL encoding the highly active TPL from *F. nucleatum*, generating the fully engineered strain *E. coli*_pPCA1_pCAT-FnTPL for TPA to L-DOPA biosynthesis. However, incubation of *E. coli*_pPCA1_pCAT-FnTPL in the presence of 5 mM TPA produced 0.99 mM catechol (20%) and no detectable L-DOPA (Fig. 2b). We hypothesized that TPL was being inhibited by upstream pathway intermediates during L-DOPA biosynthesis. Indeed, conversion of catechol to L-DOPA in *E. coli*_pFnTPL reduced from 80% to 0% when catechol was incubated in the presence of >1 mM PCA (Fig. 3d and Supplementary Fig. 6). Similar results were observed in vitro using His-tag purified FnTPL, with no L-DOPA produced at >2 mM PCA (Supplementary Fig. 6). Overall, this provided evidence to suggest the PCA-dependent inhibition of TPL during L-DOPA biosynthesis. To support this hypothesis, molecular docking simulations of catechol and PCA within the active site of FnTPL

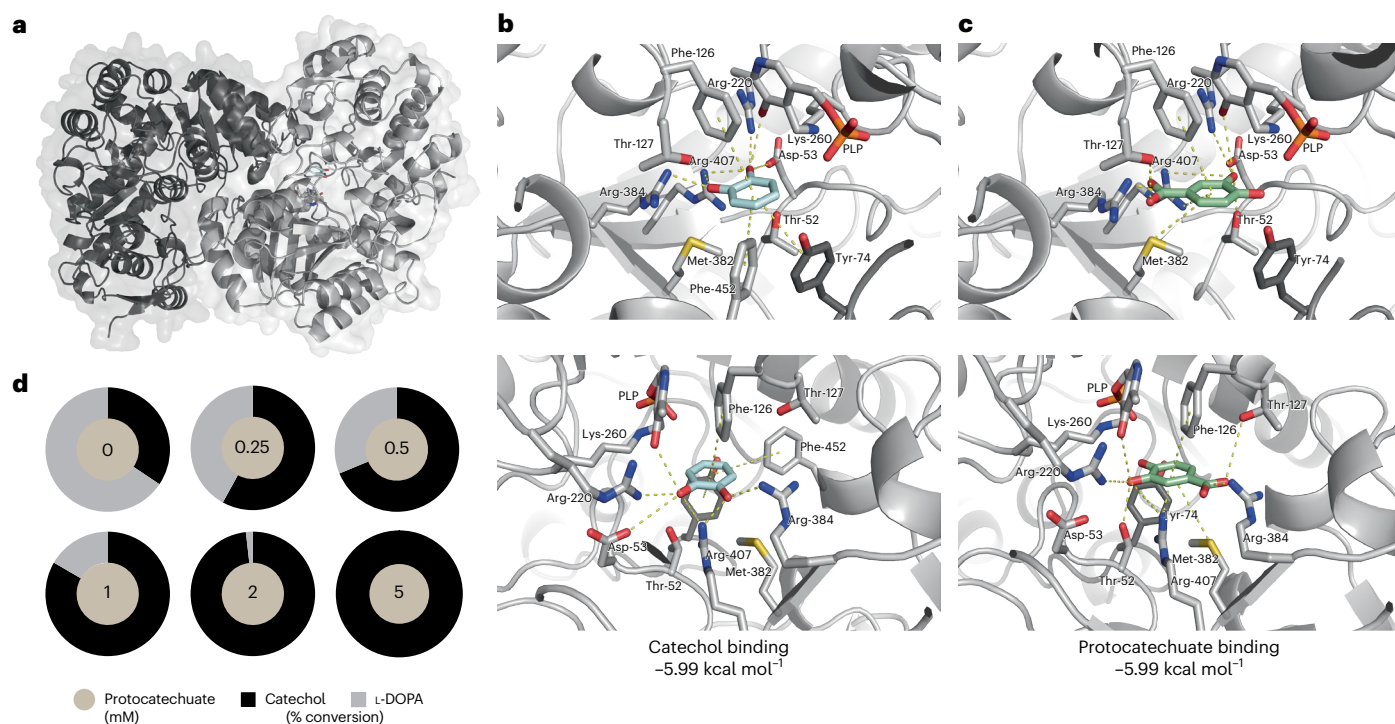


Fig. 3 | In silico modelling of TPL and in vitro inhibition by PCA. Predicted binding modes of PCA or catechol with *FtnTPL*-dimer-PLP complex. **a**, Model of the functional dimer of *FtnTPL*, with covalently linked PLP and docked catechol in monomer A (light grey) shown as stick representation in the active site. **b**, Predicted binding of catechol in the active site mediated primarily by phenylalanine and arginine residues. The catalytic Tyr-74 contributed by monomer B is highlighted in dark grey. **c**, Docked PCA bound to *FtnTPL* with interactions mediated by arginine residues augmented by Met-382, Thr-127 and

Phe-120. Both substrates are predicted to have a favourable binding affinity of $-5.99 \text{ kcal mol}^{-1}$, with Arg-220, Arg-384, Arg-407 and Thr-52 contributing to the binding of both substrates. Molecular docking simulations were performed using the molecular docking package GNINA. **d**, Assaying pathway module inhibition by pathway intermediates using *E. coli* *pFtnTPL* cells incubated in the presence of catechol and varying concentrations of PCA. Data are presented as an average of three replicate experiments to one standard deviation.

were performed using GNINA (Fig. 3). Key hydrogen bonding and electrostatic interactions were identified between PCA and conserved active site residues T127, K260, R384 and Y74. Free energy calculations showed that both PCA and catechol bind with identical and thermodynamically favourable energies ($-5.99 \text{ kcal mol}^{-1}$), suggesting that competitive binding probably occurs within the active site pocket. This aligns with recent reports of TPL inhibition by gallic acid and 3,5-dihydroxybenzoic acid in bacteria associated with mouse gut microbiota³⁵. Together, these findings provide strong evidence of PCA-dependent TPL inhibition during L-DOPA biosynthesis and highlight the need to circumvent this bottleneck to enable efficient L-DOPA production from TPA *in vivo*.

To this end, the three pathway modules were separated into two strains (*E. coli* *pPCA3_pCAT1* and *E. coli* *pFtnTPL*) to enable catechol accumulation before conversion to L-DOPA. Reaction optimizations to maximize the performance of *module 3* within *E. coli* *pFtnTPL* identified pH, time and pyruvate concentration as critical to high L-DOPA conversion from exogenous catechol in this strain (Fig. 4b). As reported in the literature³⁶, *FtnTPL* was most efficient at pH 8 (Fig. 4b). Interestingly, L-DOPA concentrations also decreased by 40% from 4.2 mM to 2.5 mM over 17 h under these optimized reaction conditions. Although L-DOPA is known to polymerize via dopaquinone to poly(dopaquinone) under aerobic conditions³⁷, the addition of antioxidants did not reverse the observed product loss over time. Liquid chromatography–mass spectrometry (LC-MS) analysis of reaction extracts instead confirmed the degradation of L-DOPA via a non-enzymatic Pictet–Spengler reaction with pyruvate to form a heterocyclic adduct (Supplementary Fig. 7)²⁷. Together, the optimum reaction conditions for L-DOPA synthesis from 5 mM catechol by *E. coli* *pFtnTPL* at $\text{OD}_{600} = 30$ were concluded to be pH 8.0 in the presence of 60 mM pyruvate for 3 h at 21 °C (Fig. 4b).

Two-strain bioconversion

Having optimized conditions for the conversion of TPA to catechol by *E. coli* *pPCA3_pCAT1* and catechol to L-DOPA by *E. coli* *pFtnTPL*, we moved on to combine these strains for the one-pot biotransformation of TPA to L-DOPA. As PCA-dependent inhibition of TPL had been observed at concentrations $>250 \mu\text{M}$, a reaction involving the sequential addition of *E. coli* *pFtnTPL* cells after incubation of *E. coli* *pPCA3_pCAT1* with TPA was envisaged. Additionally, analysis of *E. coli* *pPCA3_pCAT1* ($\text{OD}_{600} = 30$) cells incubated with 5 mM TPA at 21 °C (220 rpm) for 24 h showed $>90\%$ catechol was present in the cell supernatant, indicating this would be suitable for uptake by a second microorganism (Supplementary Fig. 8). To this end, TPA was incubated with *E. coli* *pPCA3_pCAT1* ($\text{OD}_{600} = 30$) at 21 °C (220 rpm) for 24 h, before the addition of *E. coli* *pFtnTPL* ($\text{OD}_{600} = 30$) and further incubation for 3 h. Pleasingly, this resulted in the production of L-DOPA from TPA in 0.68 g l^{-1} and 69% overall conversion as the major product by high-performance liquid chromatography (HPLC) (Fig. 4c and Supplementary Fig. 9).

CO₂ capture using microalgae

As a proof-of-concept and preliminary assessment of whether CO₂ released during the enzymatic decarboxylation of TPA to catechol could be offset, we tested whether the microalga *Chlamydomonas reinhardtii* CC1690 could recapture this CO₂ via photosynthesis. Engineered *E. coli* cultures supplied with 5 mM TPA-generated elevated CO₂ levels (Supplementary Fig. 10) and headspace gas from these cultures was transferred to actively growing *C. reinhardtii*. Within 12 h, CO₂ levels fell below the detection limit only in algal cultures and these cultures showed increased optical density and chlorophyll content relative to controls, confirming both CO₂ fixation and stimulated algal growth (Fig. 4d and Supplementary Figs. 11 and 12). While these preliminary findings suggest

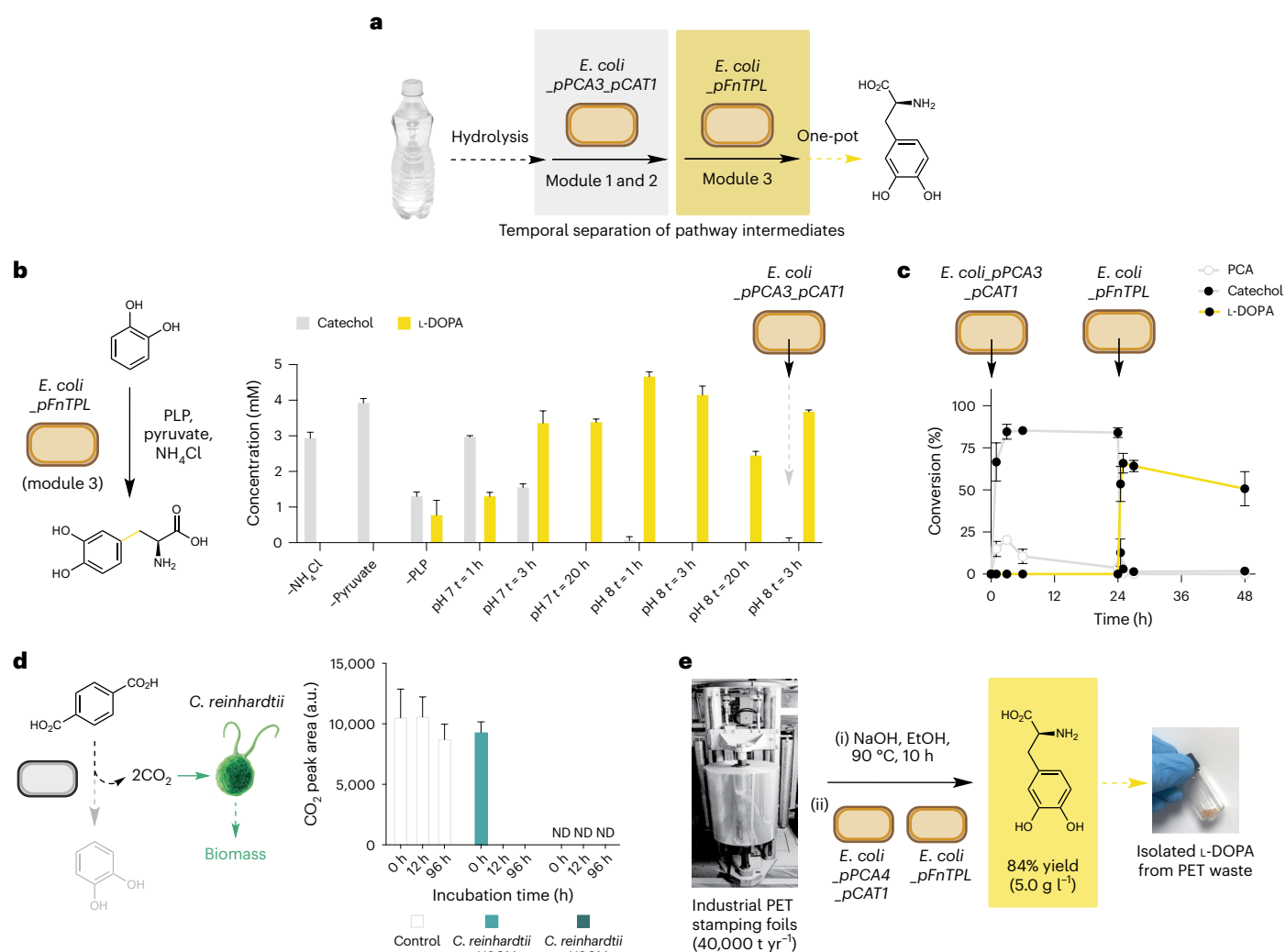


Fig. 4 | Two-strain process optimization, CO_2 capture and industrial waste upcycling. **a**, A one-pot two-strain approach to decouple PCA mediated inhibition of TPL for L-DOPA biosynthesis from TPA and PET. **b**, Whole-cell reaction optimization for conversion of exogenous catechol to L-DOPA by *E. coli* _{pFnTPL}. **c**, Time course of two strain system for conversion of TPA to L-DOPA, with 24 h of reaction from TPA to CAT by strain *E. coli* _{pPCA3_pCAT1} before addition of strain *E. coli* _{pFnTPL} for 24 h. A scaling factor of 0.83 was applied to account for dilution effects from the addition of two strains. **d**, Capture of released CO_2 from TPA whole-cell reactions in *E. coli* by *C. reinhardtii* CCI690.

Peak areas of residual CO_2 for *C. reinhardtii* grown on TAP media (control) compared with incubation with or without headspace gas mixture from *E. coli* (HSGM). **e**, Preparative microbial biosynthesis of L-DOPA salt from industrial HSF PET waste collected from API Foilmakers. Data are presented as an average of three replicate experiments to one standard deviation, except **e** which was performed as a scaled-up single replicate. Catechol was generated by strain *E. coli* _{pPCA3_pCAT1} (pH 7, 24 h, 21°C , 220 rpm) and *E. coli* _{pFnTPL} (pH 8, 3 h, 21°C , 220 rpm). Pleasingly, L-DOPA was generated from all reactions at 2.0 mM (49%) and 2.3 mM (55%) conversion from bottle and stamping foil PET waste, respectively (Supplementary Fig. 13). Furthermore, enzymatic depolymerization of PET packaging film by LCC^{JCCM} generated 4.64 mM L-DOPA from the released TPA (Supplementary Fig. 14). Reduced product conversions were attributed to the presence of lower grade PET from post-consumer waste due to residual plasticizers. The reaction was then scaled-up to 0.5 l and yielded 0.9 g l^{-1} of L-DOPA in one-pot process directly from chemically depolymerized PET waste (Supplementary Fig. 13).

that TPA-derived CO_2 can be assimilated into algal biomass, further development, quantitative analysis and system-level validation will be required to establish the extent to which coupling biosynthesis with microalgal CO_2 capture can contribute to overall process carbon neutrality.

Industrial waste valorization and product isolation

Following on from the one-pot bioconversion of PET monomer TPA to L-DOPA, we next moved on to generate L-DOPA from industrial and post-consumer PET waste. In addition to the use of a post-consumer PET bottle and packaging, we examined the upcycling of industrial PET waste. Hot stamping foils (HSF) are a prolific source of plastic waste worldwide generated by the chemical industry from the depositing of ultrathin lacquer and adhesive labels. This industry is rapidly growing (US\$2.9 billion market in 2022, 5.6% CAGR through 2032) and is estimated to generate 40,000 t of PET waste per annum globally (<https://www.maximizemarketresearch.com/market-report/global-hot-stamping-foils-market/25706>). We depolymerized a PET bottle

(from discarded waste at the University of Edinburgh, UK) and HSF samples (from API Foilmakers) under alkaline conditions, generating TPA-containing product streams that were quantified by nuclear magnetic resonance spectroscopy (51% and 83% purity for PET bottle and HSF waste, respectively). Crude TPA-rich samples were then added to optimized one-pot reactions using strains *E. coli* _{pPCA3_pCAT1} (pH 7, 24 h, 21°C , 220 rpm) and *E. coli* _{pFnTPL} (pH 8, 3 h, 21°C , 220 rpm). Pleasingly, L-DOPA was generated from all reactions at 2.0 mM (49%) and 2.3 mM (55%) conversion from bottle and stamping foil PET waste, respectively (Supplementary Fig. 13). Furthermore, enzymatic depolymerization of PET packaging film by LCC^{JCCM} generated 4.64 mM L-DOPA from the released TPA (Supplementary Fig. 14). Reduced product conversions were attributed to the presence of lower grade PET from post-consumer waste due to residual plasticizers. The reaction was then scaled-up to 0.5 l and yielded 0.9 g l^{-1} of L-DOPA in one-pot process directly from chemically depolymerized PET waste (Supplementary Fig. 13).

We next sought to isolate L-DOPA from biotransformation reactions using preparative reverse-phase HPLC. For efficient chromatographic separation, the reactions were miniaturized to generate low-volume product streams with high L-DOPA concentrations. This was achieved using a redesigned plasmid, pPCA4, which encodes *tpado*, *dcddh* and *tpaK* genes on a pBR322/rop origin backbone, compared with the p15a origin in pPCA3. This modification led to markedly improved catechol production at 30 mM TPA loading, increasing from 12.6 mM with pPCA3 to 27.6 mM with pPCA4 (Supplementary Fig. 15). In a two-step reaction involving *E. coli*_pPCA4_pCAT1 and *E. coli*_pFnTPL, we achieved 25.3 mM L-DOPA (5.0 g l⁻¹, 84% conversion) from 0.26 g of stamping foil-derived TPA following sequential incubations of 24 h (strain 1) and 3 h (strain 1 + 2) at 21 °C (Fig. 4e). L-DOPA was successfully isolated as a solid TFA salt via preparative reverse-phase HPLC, equivalent to several clinical doses typically prescribed for early-onset Parkinson's disease.

Discussion

We acknowledge that global plastic waste generation (~100 million t annually) far exceeds pharmaceutical production volumes. This pathway is therefore not proposed as a standalone solution, but rather as one component of a broader bio-upcycling portfolio. This study specifically focuses on stamping foil waste—a specialized and currently underaddressed industrial PET stream—as a viable feedstock for sustainable chemical manufacturing.

Further optimization towards industrial implementation will require pathway intensification to enable L-DOPA recovery via direct precipitation from fermentation broth, given its aqueous solubility (<5 g l⁻¹ at 20 °C)²⁶. Additional analysis will also be necessary to confirm the absence of plasticizers and other contaminants originating from stamping foil waste in the final product stream. In parallel, genomic integration of the de novo pathway will be essential to eliminate reliance on antibiotic selection at scale. This study serves as a proof-of-concept demonstration of feasibility rather than a fully optimized production process.

To enhance process sustainability, glucose recovered from surplus bread waste was shown to support biotransformation with no loss in efficiency (Supplementary Fig. 16). In addition, photosynthetic CO₂ capture by *C. reinhardtii* presents a promising route towards carbon-neutral operation, although further development is needed to fully realize this potential (Fig. 4d). Future work will focus on life-cycle and techno-economic assessments during bioreactor-scale intensification to rigorously quantify the environmental and economic benefits of the process, as well as extending the pathway towards the biosynthesis of more complex, medically relevant alkaloids from plastic waste using newly engineered microbial systems.

The conversion of waste carbon into high-value industrial chemicals remains a key objective for advancing the circular chemical and bioeconomy. This study explores the microbial transformation of TPA sourced from industrial and post-consumer PET waste into L-DOPA, a frontline medication for Parkinson's disease. A de novo biosynthetic pathway was constructed in *E. coli*, addressing design challenges related to monomer import and feedback inhibition through heterologous transporter expression and distribution across two cooperative strains. The resulting bioprocess operates under mild, aqueous conditions (pH 7–8), achieving high titres (5.0 g l⁻¹) and enabling the isolation of preparative quantities of L-DOPA from both industrial PET waste and a single post-consumer plastic bottle. Notably, the aromatic structure of the PET monomer is preserved throughout biosynthesis and embedded in the final pharmaceutical product, eliminating the need for virgin fossil carbon. Overall, this work establishes engineering biology as a route to recover and repurpose carbon from plastic waste otherwise destined for landfill, incineration or environmental pollution into high-value therapeutics for neurodegenerative disease.

Methods

Detailed methods and protocols for all experiments reported in this study are provided in Supplementary Information.

Strains and plasmids

All cloning procedures were performed in *E. coli* DH5 α . Genes encoding *tphA1A2A3*, *dcddh*, *aroY* and *kpdB* were synthesized in our previous reports^{11,12}. The *tpaK* and *tpl* genes were codon-optimized for *E. coli* BL21(DE3) and synthesized using GeneArt™ (Thermo Scientific) and His-tagged *tpl* (*hisfntpl*) used the *tpl* sequence with additional was synthesized by Integrated DNA Technologies (Supplementary Table 3). The pET21a plasmid containing *lcc* was acquired as a gift from the laboratory of C.U.

All other recombinant plasmids were constructed by homology-mediated DNA assembly or by modular cloning. Homology-mediated DNA assembly was performed using the NEBuilder HiFi DNA Assembly Cloning and modular cloning was conducted by following the JUMP protocol³⁸. Plasmids used in this study are listed in Supplementary Table 4 and were confirmed by colony PCR and Sanger sequencing (Azenta).

Oligonucleotide primers for generating plasmid pPCA3 from pPCA1 and pTpaK by homology-mediated DNA assembly were synthesized by Integrated DNA Technologies, these are pTpaK-F (tcgctgctttgagacgtactagtagcgccagctttaatacagactcactatagggggaattgtgagcgga) and pTpaK-R (cataatcctagggtgagctagccgtaaagctatcgtatgataagctgtcaaacatgagaattacaac).

Protein expression using *E. coli* BL21(DE3)

A single colony of *E. coli* BL21(DE3) cells transformed with appropriate expression plasmids was used to inoculate a 10 ml LB starter culture in a 50 ml Falcon tube containing the appropriate antibiotics and incubated overnight. For protein expression, the starter culture was back diluted to OD₆₀₀ = 0.1 in 200 ml of LB and incubated in a 500 ml Erlenmeyer flask until the OD₆₀₀ reached 0.6–0.8. At this point, isopropyl β -D-1-thiogalactopyranoside was added (final concentration of 0.5 mM) and cultured were incubated at 21 °C and 220 rpm for all proteins except *FnTPL* that was incubated at 30 °C and 220 rpm for 24 h before harvesting cells by centrifugation at 3,000g, 4 °C for whole-cell biotransformations or purification.

Whole-cell biotransformations

Harvested post-expression *E. coli* BL21(DE3) were washed with PBS, resuspended at OD₆₀₀ = 30 in M9 medium and 3 ml of the resulting cell suspension was used for each biotransformation. For TPA to PCA and PCA to CAT, disodium terephthalate or PCA (final concentration of 5 mM) and glucose (final concentration of 5% w/v, unless stated otherwise) were added and incubated in a 15 ml Falcon tube at 21 °C and 220 rpm for 24 h. For CAT to L-DOPA, CAT (final concentration of 5 mM), sodium pyruvate (60 mM), ammonium chloride (250 mM), potassium chloride (10 mM), disodium EDTA (3 mM), sodium sulfite (7 mM) and pyridoxal phosphate (1 mM) were added and incubated in a 15 ml Falcon tube at 21 °C and 220 rpm for 3 h. The supernatant was analysed by HPLC (Supplementary Table 1).

Sequestration of TPA-derived CO₂ by *C. reinhardtii*

*E. coli*_pPCA4_pCAT1 cells were resuspended in M9-glucose (2%) at OD₆₀₀ = 30 and 2.85 ml was aliquoted into headspace vials and made up to 3 ml with either 100 mM disodium terephthalate stock (5 mM final concentration) or sterile double-distilled H₂O. Vials were immediately sealed with a crimp lid and incubated (21 °C, 220 rpm, 24 h). Pregrown *C. reinhardtii* CC1690 culture in tris-acetate-phosphate (TAP) medium was aliquoted into sterile transparent glass headspace vials at a volume of 5 ml and immediately sealed with a crimp lid. To enable the transfer of evolved CO₂ from *E. coli* cultures to *C. reinhardtii* cultures or TAP control vials, *E. coli* samples were heated to 70 °C in a water bath (10 min) to increase gas abundance in the headspace. Evolved gas (15 ml) was then

drawn into a rubber-stoppered syringe through a 0.22 μm PTFE filter using a 27-gauge needle then sealed using a Luer Lock (Agilent). The needle was then sterilized by heating under a flame then evolved gas was injected into experimental samples. Pressure was applied to the septum of the crimp lid as needle was removed to promote resealing then samples were incubated under continuous illumination as previously described for desired timeframe. Gases within *E. coli*, TAP and *C. reinhardtii* samples were identified at desired timepoints by head-space gas chromatography as detailed in Supplementary Information and catechol production was analysed by HPLC.

Preparative biotransformation of PET waste TPA to L-DOPA

Step 1: 262 mg of stamping foil PET waste-derived TPA (1.50 mmol, 1.00 equiv.) was added to a suspension of fresh, PBS-washed *E. coli*_pPCA4_pCAT1 cells ($\text{OD}_{600} = 30$) in 50 ml of M9-glucose (2%) in a 500 ml Erlenmeyer flask and incubated at 21 °C, 220 rpm for 24 h. Step 2: the resulting suspension was centrifuged at 3,000g, 4 °C for 15 min and the supernatant was transferred to a 50 ml Falcon tube containing sodium pyruvate (60 mM, 2 equiv.), ammonium chloride (1 M, 33.3 equiv.), potassium chloride (10 mM), disodium EDTA (3 mM), sodium sulfite (6.8 mM) and pyridoxal phosphate (0.5 mM) before adjusting the pH to 8 using ammonium hydroxide (28% v/v, aq.). The resulting solution was used to resuspend the *E. coli*_pPCA4_pCAT1 cell pellet and then a fresh, PBS-washed (1 \times culture volume) *E. coli*_pFnTPL cell pellet (post-expression cells $\text{OD}_{600} = 30$). The resulting suspension was incubated at 21 °C, 220 rpm for 3 h (L-DOPA analytical yield of 84%) before being quenched by acidification with HCl (6 M, aq.) and then centrifuged at 3,000g, 4 °C for 15 min. Acetonitrile was added to the resulting supernatant (final concentration of 5% v/v) before being filtered (0.4 μm) and purified by prep HPLC (Teledyne LABS ACCQPrep HP150, RediSep C18, 5 μm , 18.9 ml min⁻¹, isocratic 5:95 acetonitrile + 0.1% TFA:H₂O + 0.1% TFA). Fractions containing L-DOPA were pooled and the organics were removed by rotary evaporator before lyophilization to reveal L-DOPA as the TFA salt (193 mg, 0.62 mmol, 41%).

Plastic waste hydrolysis

Chemical: PET plastic bottle waste and uncoated PET HSF waste was cleaned with 70% ethanol and cut into ~2 cm² segments. PET fragments (10 g or 20 g) were added to a mixture of 72 ml of ethanol and 288 ml of NaOH solution (10% w/v) and stirred at 90 °C for 10 h at reflux. The reaction was filtered under vacuum before the filtrate was acidified using 100 ml of HCl solution (37% aq.). The resulting white powder was collected, dried by vacuum filtration and used without further purification (Supplementary Table 5 and Supplementary Fig. 17).

Biological: PET food packaging (10 mg, cryo-milled and sorted to a sieve size of 4 mm) was incubated with purified LCC^{CCM} (3 mg of protein per g of PET waste) in 100 mM potassium phosphate buffer (pH 8.0), at 72 °C and 450 rpm for 18 h. The resulting TPA was assessed by HPLC (Supplementary Table 2).

Reporting summary

Further information on research design is available in the Nature Portfolio Reporting Summary linked to this article.

Data availability

All data supporting the findings of this study are available from the article and its Supplementary Information. Source data are provided with this paper.

References

- Zhao, X., Xiong, L., Zhang, M. & Bai, F. Towards efficient bioethanol production from agricultural and forestry residues: exploration of unique natural microorganisms in combination with advanced strain engineering. *Bioresour. Technol.* **215**, 84–91 (2016).
- Salvachúa, D., Karp, E. M., Nimlos, C. T., Vardon, D. R. & Beckham, G. T. Towards lignin consolidated bioprocessing: simultaneous lignin depolymerization and product generation by bacteria. *Green Chem.* **17**, 4951–4967 (2015).
- Kirby, J. et al. Further engineering of *R. toruloides* for the production of terpenes from lignocellulosic biomass. *Biotechnol. Biofuels* **14**, 101 (2021).
- Ma, X. et al. Upcycling chitin-containing waste into organonitrogen chemicals via an integrated process. *Proc. Natl Acad. Sci. USA* **117**, 7719–7728 (2020).
- Suitor, J. T., Varzandeh, S. & Wallace, S. One-pot synthesis of adipic acid from guaiacol in *Escherichia coli*. *ACS Synth. Biol.* **9**, 2472–2476 (2020).
- Overhage, J., Steinbüchel, A. & Priefert, H. Harnessing eugenol as a substrate for production of aromatic compounds with recombinant strains of *Amycolatopsis* sp. HR167. *J. Biotechnol.* **125**, 369–376 (2006).
- Müller, R. J., Schrader, H., Profe, J., Dresler, K. & Deckwer, W. D. Enzymatic degradation of poly(ethylene terephthalate): rapid hydrolyse using a hydrolase from *T. fusca*. *Macromol. Rapid Commun.* **26**, 1400–1405 (2005).
- Yoshida, S. et al. A bacterium that degrades and assimilates poly(ethylene terephthalate). *Science* **351**, 1196–1199 (2016).
- Bell, E. L. et al. Directed evolution of an efficient and thermostable PET depolymerase. *Nat. Catal.* **5**, 673–681 (2022).
- Lu, H. et al. Machine learning-aided engineering of hydrolases for PET depolymerization. *Nature* **604**, 662–667 (2022).
- Sadler, J. C. & Wallace, S. Microbial synthesis of vanillin from waste poly(ethylene terephthalate). *Green Chem.* **23**, 4665–4672 (2021).
- Valenzuela-Ortega, M., Suitor, J. T., White, M. F. M., Hinchcliffe, T. & Wallace, S. Microbial upcycling of waste PET to adipic acid. *ACS Cent. Sci.* **9**, 2057–2063 (2023).
- Johnson, N. W. et al. A biocompatible Lossen rearrangement in *Escherichia coli*. *Nat. Chem.* **17**, 1020–1026 (2025).
- Kim, H. T. et al. Biological valorization of poly(ethylene terephthalate) monomers for upcycling waste PET. *ACS Sustain. Chem. Eng.* **7**, 19396–19406 (2019).
- Kim, H. T. et al. Chemo-biological upcycling of poly(ethylene terephthalate) to multifunctional coating materials. *ChemSusChem* **14**, 4251–4259 (2021).
- Armijo-Galdames, B. O. & Sadler, J. C. One-pot biosynthesis of acetone from waste poly(hydroxybutyrate). *ACS Sustain. Chem. Eng.* **12**, 7748–7756 (2024).
- Bornscheuer, U. et al. Chemo-enzymatic depolymerization of functionalized low-molecular-weight polyethylene. *Angew. Chem.* **63**, e202415012 (2024).
- Sullivan, K. P. et al. Mixed plastics waste valorization through tandem chemical oxidation and biological funneling. *Science* **378**, 207–211 (2022).
- Sadler, J. C., Dennis, J. A., Johnson, N. W. & Wallace, S. Interfacing non-enzymatic catalysis with living microorganisms. *RSC Chem. Biol.* **2**, 1073–1083 (2021).
- Rabot, C. et al. Polystyrene upcycling into fungal natural products and a biocontrol agent. *J. Am. Chem. Soc.* **145**, 5222–5230 (2023).
- Koyanagi, T. et al. Effective production of 3,4-dihydroxyphenyl-L-alanine (L-DOPA) with *Erwinia herbicola* cells carrying a mutant transcriptional regulator TyrR. *J. Biotechnol.* **115**, 303–306 (2005).
- Savica, R., Grossardt, B. R., Bower, J. H., Eric Ahlskog, J. & Rocca, W. A. Time trends in the incidence of Parkinson disease. *JAMA Neurol.* **73**, 981–989 (2016).
- Tysnes, O. B. & Storstein, A. Epidemiology of Parkinson's disease. *J. Neural Transm.* **124**, 901–905 (2017).

24. Soares, A. R. et al. The role of L-DOPA in plants. *Plant Signal. Behav.* **9**, e28275 (2014).
 25. Nakagawa, A. et al. A bacterial platform for fermentative production of plant alkaloids. *Nat. Commun.* **2**, 326 (2011).
 26. Park, H. S., Lee, J. Y. & Kim, H. S. Production of L-DOPA(3, 4-dihydroxyphenyl-L-alanine) from benzene by using a hybrid pathway. *Biotechnol. Bioeng.* **58**, 339–343 (1998).
 27. Kumagai, H., Katayama, T., Koyanagi, T. & Suzuki, H. Research overview of L-DOPA production using a bacterial enzyme, tyrosine phenol-lyase. *Proc. Japan Acad. B* **99**, 75–101 (2023).
 28. Krishnaveni, R., Rathod, V., Thakur, M. S. & Neelgund, Y. F. Transformation of L-tyrosine to L-dopa by a novel fungus, *Acremonium rutilum*, under submerged fermentation. *Curr. Microbiol.* **58**, 122–128 (2009).
 29. Wei, T., Cheng, B. Y. & Liu, J. Z. Genome engineering *Escherichia coli* for L-DOPA overproduction from glucose. *Sci. Rep.* **6**, 30080 (2016).
 30. Breitel, D. et al. Metabolic engineering of tomato fruit enriched in L-DOPA. *Metab. Eng.* **65**, 185–196 (2021).
 31. Patrauchan, M. A. et al. Catabolism of benzoate and phthalate in *Rhodococcus* sp. strain RHA1: redundancies and convergence. *J. Bacteriol.* **187**, 4050–4063 (2005).
 32. Salvador, M. et al. Microbial genes for a circular and sustainable bio-PET economy. *Genes* **10**, 373 (2019).
 33. Schweigert, N., Zehnder, A. J. B. & Eggen, R. I. L. Chemical properties of catechols and their molecular modes of toxic action in cells, from microorganisms to mammals. *Environ. Microbiol.* **3**, 81–91 (2001).
 34. Li, Q., Aubrey, M. T., Christian, T. & Freed, B. M. Differential inhibition of DNA synthesis in human T cells by the cigarette tar components hydroquinone and catechol. *Fundam. Appl. Toxicol.* **38**, 158–165 (1997).
 35. Kobayashi, T. et al. 3,5-Dihydroxybenzoic acid as a potent inhibitor of tyrosine phenol-lyase decreases fecal phenol levels in mice. *J. Med. Chem.* **68**, 8786–8795 (2025).
 36. Tang, X. L. et al. Process development for efficient biosynthesis of L-DOPA with recombinant *Escherichia coli* harboring tyrosine phenol lyase from *Fusobacterium nucleatum*. *Bioprocess. Biosyst. Eng.* **41**, 1347–1354 (2018).
 37. Zhang, X. et al. Endogenous 3,4-dihydroxyphenylalanine and dopaquinone modifications on protein tyrosine: links to mitochondrially derived oxidative stress via hydroxyl radical. *Mol. Cell. Prot.* **9**, 1199–1208 (2010).
 38. Valenzuela-Ortega, M. & French, C. Joint universal modular plasmids (JUMP): a flexible vector platform for synthetic biology. *Synth. Biol.* **6**, ysab003 (2021).
- C.U. acknowledges NSRF funding via the Research and Innovation Acceleration Agency for Competitiveness and Area Development (RCAD) (Program Management Unit for Technology and Innovation for Future Industries (PMU-B): Brainpower for Future Industries; grant number B38G690002). B.E. acknowledges research assistant and studentship funds from VISTEC. We thank G. Leung and T. Hinchcliffe (Impact Solutions) for insightful discussions, B. French (API Foilmakers) for providing HSF samples, C. P. Lilly and A. Molnar for providing a strain of *C. reinhardtii* CC1690 and experimental assistance and R. Cox (C-Source Renewables) for supplying bread waste glucose syrups.

Author contributions

The study was designed by S.W. and B.R. Experimental work was performed and analysed by B.R., Y.E., M.V.-O., T.W.T., C.L.T., K.C., J.F.C.S., N.Z., E.S.-P. and B.E. C.U., C.W.W. and S.W. provided project support and experimental guidance. The paper was written by S.W., B.R., Y.E., M.V.-O., T.W.T., C.L.T., K.C., J.F.C.S. and E.S.-P. All authors have given approval to the final version of the paper.

Competing interests

The authors declare no competing interests.

Additional information

Supplementary information The online version contains supplementary material available at <https://doi.org/10.1038/s41893-026-01785-z>.

Correspondence and requests for materials should be addressed to Stephen Wallace.

Peer review information *Nature Sustainability* thanks the anonymous reviewers for their contribution to the peer review of this work.

Reprints and permissions information is available at www.nature.com/reprints.

Publisher's note Springer Nature remains neutral with regard to jurisdictional claims in published maps and institutional affiliations.

Open Access This article is licensed under a Creative Commons Attribution 4.0 International License, which permits use, sharing, adaptation, distribution and reproduction in any medium or format, as long as you give appropriate credit to the original author(s) and the source, provide a link to the Creative Commons licence, and indicate if changes were made. The images or other third party material in this article are included in the article's Creative Commons licence, unless indicated otherwise in a credit line to the material. If material is not included in the article's Creative Commons licence and your intended use is not permitted by statutory regulation or exceeds the permitted use, you will need to obtain permission directly from the copyright holder. To view a copy of this licence, visit <http://creativecommons.org/licenses/by/4.0/>.

© The Author(s) 2026

Acknowledgements

B.R. acknowledges a PhD studentship from the Industrial Biotechnology Innovation Centre (IBiolC). S.W. acknowledges a Future Leaders Fellowship from UKRI (MR/S033882/1), Sustainable Manufacturing grant from EPSRC (EP/W019000/1), Engineering Biology Mission Hub grant from BBSRC (BB/Y007972/1) and Sustainable Manufacturing Hub grant (UKRI1891). C.W.W. acknowledges a sLOLA grant from BBSRC (BB/X003027/1).

Reporting Summary

Nature Portfolio wishes to improve the reproducibility of the work that we publish. This form provides structure for consistency and transparency in reporting. For further information on Nature Portfolio policies, see our [Editorial Policies](#) and the [Editorial Policy Checklist](#).

Statistics

For all statistical analyses, confirm that the following items are present in the figure legend, table legend, main text, or Methods section.

n/a Confirmed

- The exact sample size (n) for each experimental group/condition, given as a discrete number and unit of measurement
- A statement on whether measurements were taken from distinct samples or whether the same sample was measured repeatedly
- The statistical test(s) used AND whether they are one- or two-sided
Only common tests should be described solely by name; describe more complex techniques in the Methods section.
- A description of all covariates tested
- A description of any assumptions or corrections, such as tests of normality and adjustment for multiple comparisons
- A full description of the statistical parameters including central tendency (e.g. means) or other basic estimates (e.g. regression coefficient) AND variation (e.g. standard deviation) or associated estimates of uncertainty (e.g. confidence intervals)
- For null hypothesis testing, the test statistic (e.g. F , t , r) with confidence intervals, effect sizes, degrees of freedom and P value noted
Give P values as exact values whenever suitable.
- For Bayesian analysis, information on the choice of priors and Markov chain Monte Carlo settings
- For hierarchical and complex designs, identification of the appropriate level for tests and full reporting of outcomes
- Estimates of effect sizes (e.g. Cohen's d , Pearson's r), indicating how they were calculated

Our web collection on [statistics for biologists](#) contains articles on many of the points above.

Software and code

Policy information about [availability of computer code](#)

Data collection

Data analysis

For manuscripts utilizing custom algorithms or software that are central to the research but not yet described in published literature, software must be made available to editors and reviewers. We strongly encourage code deposition in a community repository (e.g. GitHub). See the Nature Portfolio [guidelines for submitting code & software](#) for further information.

Data

Policy information about [availability of data](#)

All manuscripts must include a [data availability statement](#). This statement should provide the following information, where applicable:

- Accession codes, unique identifiers, or web links for publicly available datasets
- A description of any restrictions on data availability
- For clinical datasets or third party data, please ensure that the statement adheres to our [policy](#)

All data supporting the findings of this study are available from the article and its Supplementary Information files. Source data are provided with this paper.

Research involving human participants, their data, or biological material

Policy information about studies with [human participants or human data](#). See also policy information about [sex, gender \(identity/presentation\), and sexual orientation](#) and [race, ethnicity and racism](#).

Reporting on sex and gender	n/a
Reporting on race, ethnicity, or other socially relevant groupings	n/a
Population characteristics	n/a
Recruitment	n/a
Ethics oversight	n/a

Note that full information on the approval of the study protocol must also be provided in the manuscript.

Field-specific reporting

Please select the one below that is the best fit for your research. If you are not sure, read the appropriate sections before making your selection.

Life sciences Behavioural & social sciences Ecological, evolutionary & environmental sciences

For a reference copy of the document with all sections, see [nature.com/documents/nr-reporting-summary-flat.pdf](https://www.nature.com/documents/nr-reporting-summary-flat.pdf)

Life sciences study design

All studies must disclose on these points even when the disclosure is negative.

Sample size	A sample size of three independent biological replicates was chosen.
Data exclusions	No data was excluded from the study.
Replication	All data was performed in triplicate with appropriate negative or positive controls and all replicates were successful.
Randomization	Randomization was not performed and is not relevant to the study as observations would not have been affected by group randomization due to lack of animal subjects and nature of measurements.
Blinding	Blinding was not performed and is not relevant to the study as observations would not have been affected by group randomization due to lack of animal subjects and nature of measurements.

Reporting for specific materials, systems and methods

We require information from authors about some types of materials, experimental systems and methods used in many studies. Here, indicate whether each material, system or method listed is relevant to your study. If you are not sure if a list item applies to your research, read the appropriate section before selecting a response.

Materials & experimental systems

n/a	Involvement in the study
<input checked="" type="checkbox"/>	<input type="checkbox"/> Antibodies
<input checked="" type="checkbox"/>	<input type="checkbox"/> Eukaryotic cell lines
<input checked="" type="checkbox"/>	<input type="checkbox"/> Palaeontology and archaeology
<input checked="" type="checkbox"/>	<input type="checkbox"/> Animals and other organisms
<input checked="" type="checkbox"/>	<input type="checkbox"/> Clinical data
<input checked="" type="checkbox"/>	<input type="checkbox"/> Dual use research of concern
<input checked="" type="checkbox"/>	<input type="checkbox"/> Plants

Methods

n/a	Involvement in the study
<input checked="" type="checkbox"/>	<input type="checkbox"/> ChIP-seq
<input checked="" type="checkbox"/>	<input type="checkbox"/> Flow cytometry
<input checked="" type="checkbox"/>	<input type="checkbox"/> MRI-based neuroimaging

Plants

Seed stocks

n/a

Novel plant genotypes

n/a

Authentication

n/a